

PDGF-B Can Sustain Self-renewal and Tumorigenicity of Experimental Glioma-Derived Cancer-Initiating Cells by Preventing Oligodendrocyte Differentiation^{1,2}

Yiwen Jiang, Maria Boije, Bengt Westermark and Lene Uhrbom

Department of Immunology, Genetics and Pathology, Rudbeck Laboratory, Uppsala University, Uppsala, Sweden

Abstract

According to the cancer stem cell (CSC)/cancer-initiating cell hypothesis, glioma development is driven by a subpopulation of cells with unique tumor-regenerating capacity. We have characterized sphere-cultured glioma-derived cancer-initiating cells (GICs) from experimental gliomas induced by platelet-derived growth factor-B (PDGF-B) in neonatal *Gtv-a Arf^{-/-}* mice. We found that the GICs can maintain their stem cell-like characteristics in absence of exogenous epidermal growth factor and fibroblast growth factor 2 and that this culture condition was highly selective for tumor-initiating cells where as few as five GICs could induce secondary tumor formation after orthotopic transplantation. Addition of FBS to the medium caused the GICs to differentiate into cells coexpressing glial fibrillary acidic protein and Tuj1, and this differentiation process was reversible, suggesting that the GICs are highly plastic and able to adapt to different environments without losing their tumorigenic properties. On inhibition of virally transduced PDGF-B by small interfering RNA treatment, the GICs stopped proliferating, lost their self-renewal ability, and started to uniformly express CNPase, a marker of oligodendrocyte precursor cells and mature oligodendrocytes. Most importantly, PDGF-B depletion completely abrogated the tumor-initiating capacity of the GICs. Our findings suggest that interfering with PDGF-controlled differentiation could be a therapeutic avenue for patients diagnosed with the PDGF-driven proneural subtype of human glioblastoma.

Neoplasia (2011) 13, 492–503

Introduction

Glioma is the most frequent primary tumor of the central nervous system. Gliomas are divided into grades 1 to 4 based on malignancy according to the World Health Organization classification. The prognosis of a grade 4 glioma, glioblastoma, remains dismal with a median survival of about 12 to 15 months, and there is as yet no cure [1]. Large-scale genomic characterization of human glioblastoma has revealed three core signaling pathways that are altered in most tumors: the receptor tyrosine kinase (RTK)/RAS/PI3K, the p53, and the RB signaling pathways [1,2]. The most common alterations leading to activation of RTKs are *EGFR* amplifications and *PDGFRA* amplifications. Further, global gene expression analysis has revealed four new subclasses of glioblastoma based on their expression profiles: proneural, neural, classic, and mesenchymal [3]. The proneural subtype is associated with *PDGFRA* abnormalities and *IDH1* and *TP53* mutations. This group also has a high expression of genes involved in

oligodendrocytic development such as *OLIG2* and *SOX2*. Unlike the classic subtype, associated with high-level *EGFR* amplification and frequent *CDKN2A* deletion, and the mesenchymal subtype, associated with frequent *NF1* deletions, where mortality was significantly

Address all correspondence to: Lene Uhrbom, PhD, Department of Immunology, Genetics and Pathology, Rudbeck Laboratory, Uppsala University, SE-75185 Uppsala, Sweden. E-mail: lene.uhrbom@igp.uu.se

¹This work has been supported by grants from the Swedish Cancer Society, the Swedish Research Council, the Association for International Cancer Research, the Swedish Childhood Cancer Foundation, and the Swedish Society of Medicine.

²This article refers to supplementary material, which is designated by Figure W1 and is available online at www.neoplasia.com.

Received 16 February 2011; Revised 24 March 2011; Accepted 28 March 2011

Copyright © 2011 Neoplasia Press, Inc. All rights reserved 1522-8002/11/\$25.00
DOI 10.1593/neo.11314

reduced in response to intense chemotherapy and radiotherapy, the proneural subtype did not respond well to these therapies [3].

A large body of evidence has emerged suggesting that human glioma contains glioma-derived cancer-initiating cells (GICs), a minor cell population with unique capacity to regenerate brain tumors *in vivo* with maintained characteristics of the primary tumor. GICs express many markers associated with neural stem cells (NSCs) such as nestin, SOX2, Bmi-1, Notch, and Jagged [4–7]. When cultured under stem cell conditions, GICs have the capacity of extended self-renewal as spheres, as well as the ability to differentiate into multiple neural cell lineages *in vitro*. Initially, GICs were isolated based on CD133 expression, which was believed to be a unique marker for GICs [6]. Subsequent studies have shown that there are both CD133⁺ and CD133⁻ GICs, thus CD133 is not an obligatory marker for GICs [8,9]. GICs have been shown to have increased resistance to radiotherapy by activation of the DNA damage response pathway [10] and to chemotherapy through efflux of drugs through the ABCG2 transporter [11]. Collectively, this makes GICs a vital target for new therapeutic strategies for glioma.

The central role of platelet-derived growth factor (PDGF) in the development of glioma suggests that PDGF signaling is important for GIC initiation and maintenance. We have studied the properties of GICs derived from experimental gliomas that show many similarities to the proneural subtype of glioblastoma. We used the RCAS/TV-A (replication-competent avian leukosis virus splice acceptor/avian leukosis virus receptor) somatic cell gene transfer mouse model of glioma, and intracerebral tumors were induced by RCAS-PDGF-B in neonatal *Gtv-a* (GFAP-*tv-a*) *Arf*^{-/-} mice. Generated gliomas display histopathologic features of glioblastoma and expression of PDGFRA, OLIG2, and SOX2 that are connected to the proneural subtype of glioblastoma [12]. GICs were isolated and cultured as neurospheres in defined medium without addition of growth factors. As reference cells, normal NSCs were isolated from *Gtv-a Arf*^{-/-} mice and cultured in defined NSC medium. The role of PDGF signaling for fundamental features of GICs such as self-renewal, proliferation, differentiation, and *in vivo* tumorigenesis has been studied, and we show that PDGF-B is necessary for stemness and tumorigenicity of GICs by preventing them from differentiating.

Materials and Methods

Infection of Transgenic Mice

Gtv-a Arf^{-/-} mice were used to generate the primary brain tumors. Neonatal mice were injected in the right cerebral hemisphere with 2 μ l of DF-1 chicken fibroblasts producing RCAS-PDGF-B-HA as described [13]. Infected mice were monitored every second day and killed on any sign of illness. All animal experiments were performed in accordance with the rules and regulations of Uppsala University and were approved by the local animal ethics committee.

Histopathology and Immunofluorescence Analyses of Tumors

The brains of sick mice were taken out and cut coronally at the injection site. The anterior piece was used for neurosphere culture. For primary tumors, the posterior piece was fixed in 4% paraformaldehyde for 1 hour, then cryoprotected in 30% sucrose overnight, both at 4°C, and finally embedded in OCT and frozen. The posterior piece from secondary tumors was fixed in 4% formalin for at least 48 hours, embedded in paraffin, sectioned, and analyzed for the presence of tumor tissue by viewing hematoxylin and eosin (H&E)-stained sections. Tissue sections were blocked in PBS contain-

ing Triton X-100 (PBS-T) and 5% milk. Primary antibodies against HA (1:100; Abcam, Cambridge, UK), Ki67 (1:100; Dako, Glostrup, Denmark), Olig2 (1:200; Millipore, Temecula, CA), Nestin (1:200; BD Bioscience, Franklin Lakes, NJ), and glial fibrillary acidic protein (GFAP; 1:400; Dako) were incubated in blocking solution at 4°C overnight. The sections were then washed with PBS-T three times and incubated with secondary antibodies donkey antirabbit Alexa 488 (1:400; Invitrogen, Carlsbad, CA), donkey antimouse Alexa 555 (1:400; Invitrogen), and goat antirat Alexa 555 (1:400; Invitrogen) in PBS-T at room temperature for 1 hour. After final washing three times in PBS-T, sections were mounted in Immu-mount (Thermo-Scientific, Waltham, MA) with 4',6-diamidino-2-phenylindole.

Neurosphere Culture

Tumor tissue was extracted using a scalpel, trying to remove as much of the normal tissue as possible, minced with the scalpel, and incubated in Accutase (eBioscience, San Diego, CA) for 15 minutes at 37°C. Tissue pieces were washed three times in Dulbecco modified Eagle medium (DMEM; Sigma, Hamburg, Germany) followed by trituration using a 1000- μ l pipette. Cells were passed through a 70- μ m cell strainer and seeded into six-well tissue culture plates. Cells were grown in GIC medium containing DMEM-F12 GlutaMAX (GIBCO-Invitrogen), 1% penicillin G/streptomycin sulfate (Sigma), B-27 without vitamin A (1:50; GIBCO-Invitrogen), HEPES (0.2 mM; Sigma), and insulin (20 ng/ml; Sigma). Spheres were passaged by trituration through a 1000- μ l pipette and reseeded into fresh medium. Sphere cultures below passage 25 were used for all analyses described in this article. As reference cells, brain tissue from uninjected *Gtv-a Arf*^{-/-} mice was dissociated the same way as the tumor tissue. NSCs were cultured in NSC medium, which is GIC medium supplemented with fibroblast growth factor 2 (FGF2, 20 ng/ml; PeproTech, Rocky Hill, NJ) and epidermal growth factor (EGF, 20 ng/ml; PeproTech).

Intracranial Cell Transplantation into Syngeneic Mice

Spheres were dissociated by trituration through a 1000- μ l pipette, and the number of cells was determined using a Coulter Counter (Coulter Electronics, Herpendon, UK). The appropriate number of cells was resuspended in DMEM/F12 medium to reach a total cell count of 5, 50, 500, and 5000 (tumor cells) or 500,000 (control cells) per 2- μ l medium, respectively. From these aliquots, 2 μ l was orthotopically injected into neonatal syngeneic mice. Injected mice were monitored every second day. The brains of sick mice were taken out and subjected to histopathology analyses as described previously.

Sphere-Forming Assay

Spheres were dissociated into single cells and seeded at a density of 50 cells/well in a 96-well plate under different culture conditions. The cells were left undisturbed and cultured for 7 days. On day 7, pictures of cultured cells were taken using a phase-contrast microscope (Olympus Europa GmbH, Hamburg, Germany). The experiment was repeated twice.

Limiting Dilution Assay

Limiting dilution assay was performed as described previously [14]. Spheres were dissociated into single cells and plated in 96-well plates in 0.2 ml of GIC medium containing different combinations of growth factors. Final cell numbers ranged from 400 cells/well to 1 cell/well. Cultures were left undisturbed for 10 days, and then the

percentage of wells not containing spheres for each cell dilution was calculated and plotted against the number of cells per well. Linear regression lines were plotted, and the number of cells required to generate at least one sphere in every well (=the stem cell frequency) was calculated. The experiment was repeated twice.

Differentiation Assay

Small spheres (formed after 2 days of passaging) were seeded onto extracellular matrix– (1:5; Sigma) coated glass coverslips in individual wells of a 24-well plate. The cells were cultured in NSC medium, GIC medium, or GIC medium with 5% FBS (Sigma) for 7 days before analysis. Medium was changed once after 3 to 4 days of culturing. For quantification of cell markers, more than 300 cells for each condition were counted. The experiment was repeated three times. In the differentiation reversibility assay, bromodeoxyuridine (BrdU) was added 16 hours before fixation.

RNA Interference of Viral Produced Human PDGF-B

Small spheres were dissociated into single cells and seeded into six-well plates. Cells were transfected with control small interfering RNA (siRNA) or siRNA against human PDGF-B messenger RNA (Dharmacon, Lafayette, CO) that was specifically selected not to hybridize to mouse PDGF-B messenger RNA. Transfection was performed according to the manufacturer's manual. Forty-eight hours after transfection, cells were either dissociated and seeded for limiting dilution assay or seeded on ECM- (1:5; Sigma) coated glass coverslips for a second round of transfection. These cells were fixed after another 48 hours of transfection in 4% paraformaldehyde, and immunofluorescence analysis was performed. BrdU was added to the cells 16 hours before fixation. For BrdU quantification, more than 300 cells were counted for each transfection. The experiment was repeated three times.

Immunocytochemical Analyses

Cells were fixed in 4% paraformaldehyde for 10 minutes. After washing in PBS, cells were treated with 0.2% Triton X-100 and blocked for 1 hour in a solution containing 1% BSA and 5% normal goat serum. Primary antibodies against GFAP (1:400; Dako), Tuj1 (1:400; Covance, Princeton, NJ), CNP (1:400; Covance), nestin (1:100; BD Bioscience), SOX2 (1:500; Millipore), HA (1:40; Santa Cruz Biotechnologies, Santa Cruz, CA), PDGFR α (1:100; Santa Cruz Biotechnologies), BrdU (1:100; Abcam), Ki67 (1:100; Dako), or Caspase-3 (1:100; Chemicon, Billerica, MA) were incubated overnight in a humidified chamber at 4°C. Coverslips were washed three times in PBS and incubated with the secondary antibodies donkey antirabbit Alexa 488 (1:400; Invitrogen), donkey antimouse Alexa 555 (1:400; Invitrogen), and goat antirat (1:400; Invitrogen) for 1 hour at room temperature. Coverslips were then washed three times in PBS and mounted in Immu-mount (Thermo-Scientific) containing 0.1% DAPI.

Results

GIC Self-renewal In Vitro Was Independent of Exogenous Mitogens

To investigate the properties of experimental GICs, gliomas were induced with RCAS-PDGFB-HA in neonatal *Gtv-a Arf^{-/-}* mice. The *Arf^{-/-}* background was chosen because it is one of the most common mutations of human glioblastoma found in more than 50% of proneural tumors [3], and in experimental gliomas, it increases tumor incidence and malignancy [12]. Until now, most stud-

ies on experimental and human GICs have been carried out under the same culture conditions as for normal NSCs, that is, in defined medium containing EGF and FGF2 [14]. However, NSCs are prone to migrate toward glioma lesions [15] making it difficult to avoid contaminating the GIC cultures with NSCs. In our initial experiments, explanted tumor cells were cultured under regular NSC conditions, but we soon experienced, by staining for HA (expression of retroviral PDGF-B) that, after a few passages, normal NSCs had completely taken over the culture (data not shown). On removal of EGF and FGF2 from the NSC medium, we found that the GICs could be enriched for and stably maintained. Therefore, in this investigation, we have used tumor sphere cultures derived from PDGF-B–induced glioblastoma-like tumors cultured in GIC medium (NSC medium without EGF and FGF2). Spheres could be observed after 7 days in cultures from five different tumors (TS1-TS5). The TS1 and TS2 cells were used throughout this investigation. As reference cells, we have used neurospheres (NS1) derived from uninjected *Gtv-a Arf^{-/-}* mice. The NS1 cells were cultured in NSC medium because they could not be established or expanded in GIC medium or GIC medium with addition of exogenous PDGF-BB.

To analyze the self-renewal capacity of NSCs and GICs in response to different combinations of exogenous growth factors, NS1 and TS1 cells were seeded at clonal density (1000 cells/ml) in GIC medium with or without the addition of EGF, FGF2, or PDGF-BB (Figure 1, A–I). After 7 days, NS1 cells had the ability to form spheres only when EGF was present (Figure 1, A–E). TS1 cells, however, could form spheres under all conditions (Figure 1, F–J).

Limiting dilution assay was performed to estimate the stem cell frequency of TS1 and NS1 cultures under the same conditions as in the sphere formation assay. The number of NS1 cells required to generate at least one sphere/well was around 8 for both EGF and EGF + FGF2 (Figure 1J) and 9 for TS1 cells in all conditions tested: EGF, EGF + FGF2, FGF2, and no growth factors (Figure 1K). Thus, the tumor-derived cells and the corresponding normal NSCs contained similar frequencies of cells with self-renewal capacity, but the tumor-derived cells could be distinguished from the NSCs by their ability to self-renew independently of exogenous EGF and FGF2.

The mechanism behind the growth factor independence of TS cells was investigated by analyzing PDGFR- α and PDGFR- β expression in NS1 and TS1 cells. No PDGF receptors were expressed by the NS1 cells (Figure 1, L and N), explaining why NS1 cells could not respond to exogenous PDGF-B (Figure 1E). In contrast, TS1 cells expressed high levels of PDGFR- α (Figure 1M) but had no expression of PDGFR- β (Figure 1O).

Tumor-Derived Sphere Cells Could Induce Secondary Gliomas

A fundamental characteristic of CSCs/cancer-initiating cells (CICs) is that they must be able to generate secondary tumors on orthotopic transplantation. To analyze the tumor-initiating ability of the tumor-derived cells, TS1 cells were orthotopically transplanted into newborn syngeneic mice. Spheres from TS1 cells were dissociated into single cells, and 5, 50, 500, or 5000 cells were injected intracerebrally after which the mice were monitored for 12 weeks (Figure 1P). Mice that had received 5000 TS1 cells ($n = 10$) started to show signs of illness 20 days after transplantation, and all mice presented with tumors within 40 days. On injection of 500 TS1 cells ($n = 10$), 90% of the mice developed tumors, and the latency was longer. Injection of 50 TS1 cells ($n = 14$) caused a tumor incidence of 21% and injection of 5 TS1 cells ($n = 12$) initiated tumors in 33%

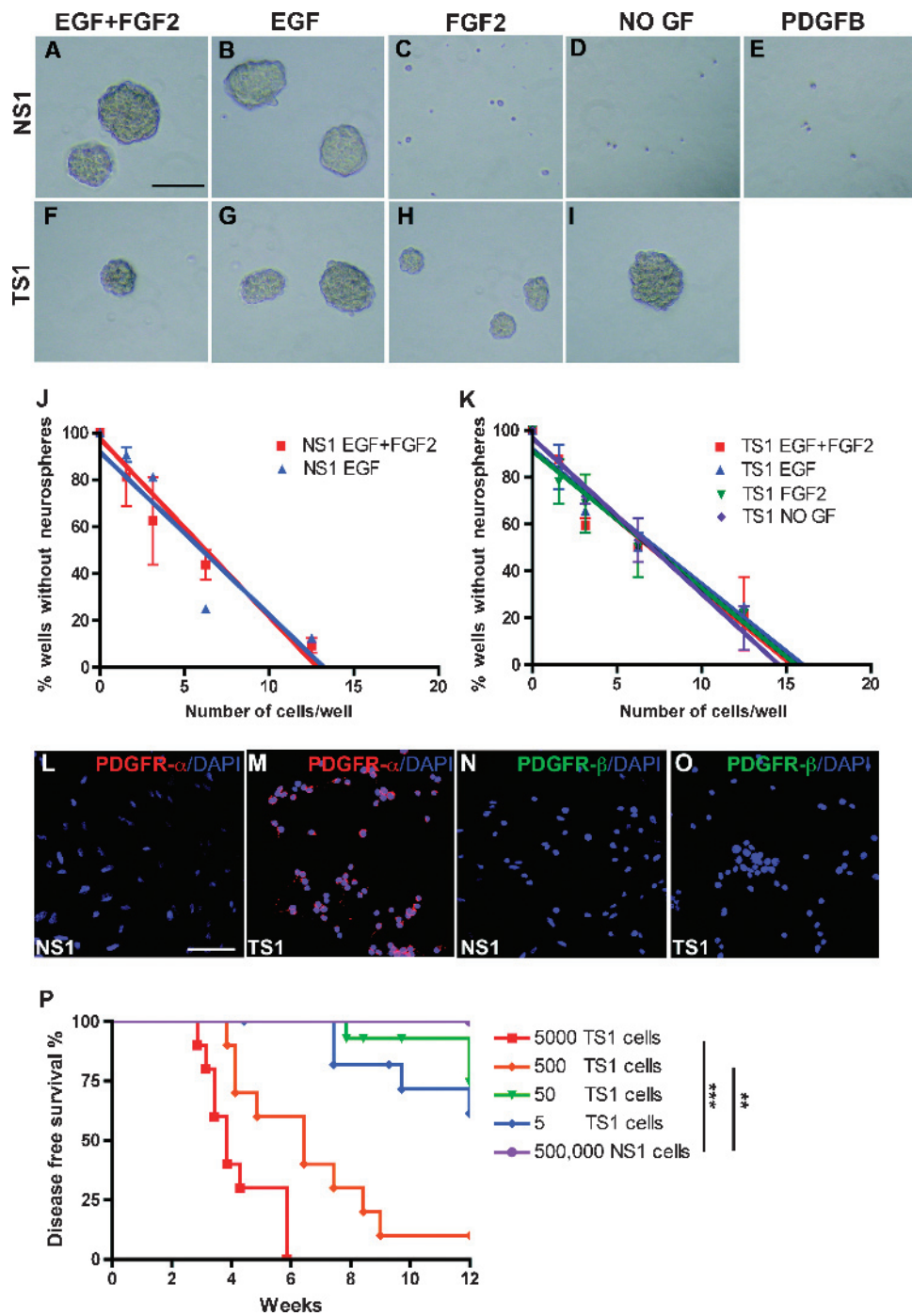


Figure 1. Self-renewal, stem cell frequency, and tumorigenicity of glioma-derived tumor sphere cells. (A-E) Sphere-forming assay showing the ability of NSCs (A-E; NS1 cells) and TS1 (F-I) cells to generate spheres in GIC medium containing different combinations of growth factors. Scale bar, 50 μ m. (J-K) The result from the limiting dilution assay showing linear regression curves to determine the stem cell frequency in NS1 (J) and TS1 (K) cells. The experiments were repeated twice. (L-O) Immunofluorescence staining for PDGFR- α and PDGFR- β in NS1 and TS1 cells. Scale bar, 50 μ m. (P) Kaplan-Meier graph showing survival of Gtv-a *Ar^{f-/-}* mice orthotopically transplanted with 5000, 500, 50, or 5 TS1 cells or 500,000 NS1 cells. Log-rank test, ** $P < 0.01$, *** $P < 0.001$.

of the mice. In contrast, mice injected with 500,000 NSCs (NS1) were 100% tumor free after 12 weeks of injection ($n = 6$). There was a significant difference in survival between NS1-injected mice and mice injected with 5000 TS1 cells (Fisher exact test, $P = .0003$) or 500 TS1 cells (Fisher exact test, $P = .0011$), respectively.

Histopathologic analysis of the primary tumor from which the TS1 cells were derived (Figure W1A) and the secondary tumors gener-

ated by TS1 cells (Figure W1B) showed several features of glioblastoma including areas of pseudopalisading necrosis (Figure W1A, H&E) and microvascular proliferations (Figure W1B, H&E). All secondary tumors were of grade 4 malignancy with high cellular density. Immunostainings of the primary tumor and one representative secondary tumor showed that both were positive for HA (Figure W1, A and B, HA), confirming that the secondary tumor had originated from the transplanted TS1

cells. Primary and secondary tumors were Ki67 positive, with notably more positive cells in the secondary tumor (Figure W1, *A* and *B*, Ki67). Tumors were also positive for Olig2, nestin, and GFAP (Figure W1, *A* and *B*). Because the glioma-derived TS1 cells were highly capable of inducing brain tumors with many features similar to the primary tumor, they could be regarded as true GICs.

GICs Exhibited Aberrant Differentiation Capacity

In addition to extended self-renewal and tumor-initiating capabilities, GICs should hold the potential to differentiate into glial and

neuronal cell types. First, we analyzed the expression of NSC markers nestin and SOX2 in GICs and NSCs. Small spheres of NS1, TS1, and TS2 cells were seeded onto ECM-coated coverslips and cultured for 7 days in NSC medium, GIC medium, or GIC medium with addition of 5% fetal bovine serum. Serum has previously been used to show that human GICs are capable of multilineage differentiation [5]. Cells migrated out from the neurospheres and formed a monolayer on the coverslips that could be subjected to immunofluorescence analyses. When NSCs and GICs were cultured in NSC medium, they exhibited an immature, bipolar morphology and were strongly

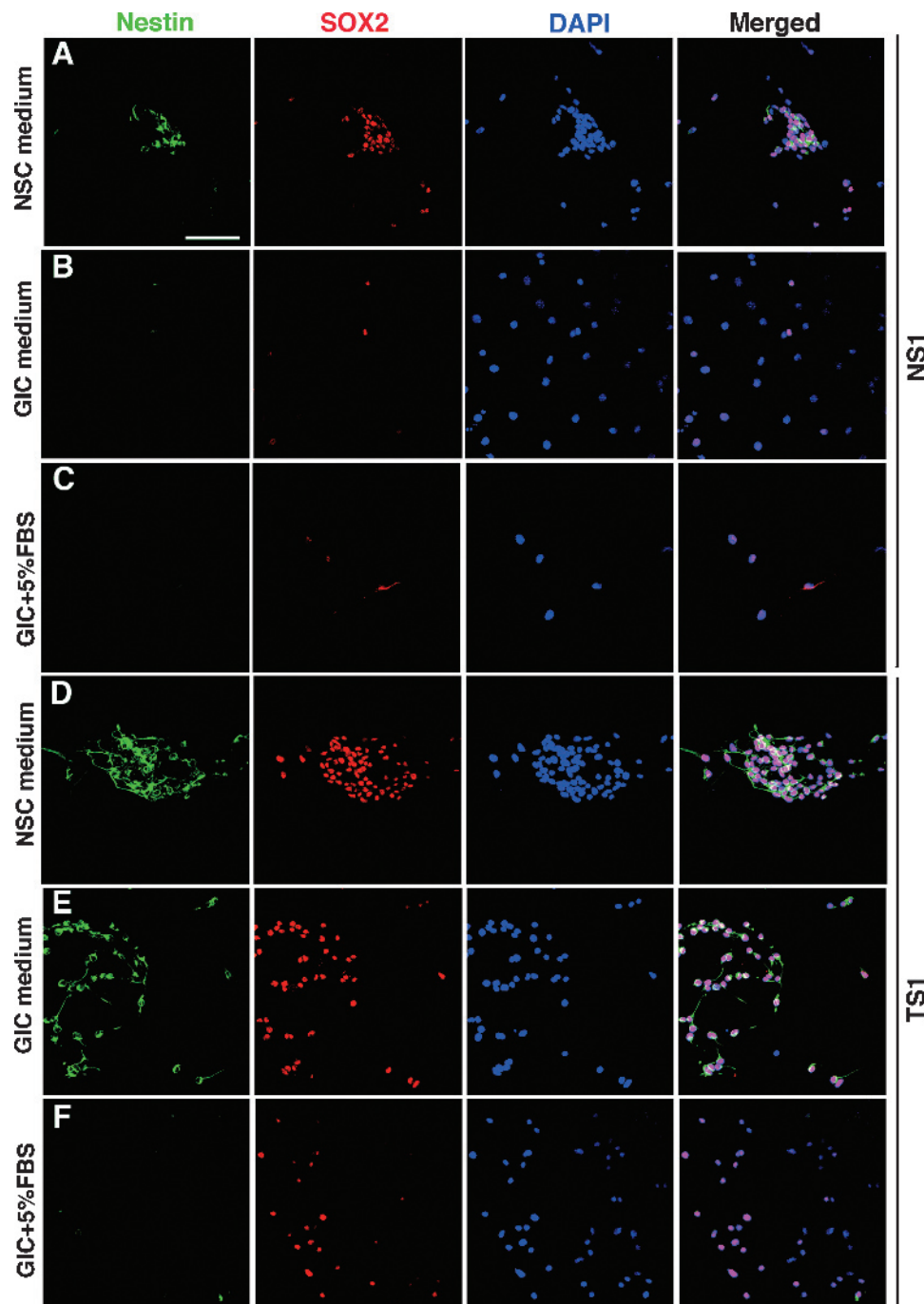


Figure 2. Expression of nestin and SOX2 in representative samples of NS1 and TS1 cells under different culture conditions for 7 days. NSCs cultured in NSC medium (A), GIC medium (B), or GIC medium + 5% FBS (C) and GICs cultured in NSC medium (D), GIC medium (E), or GIC medium + 5% FBS (F). Scale bar, 50 μ m.

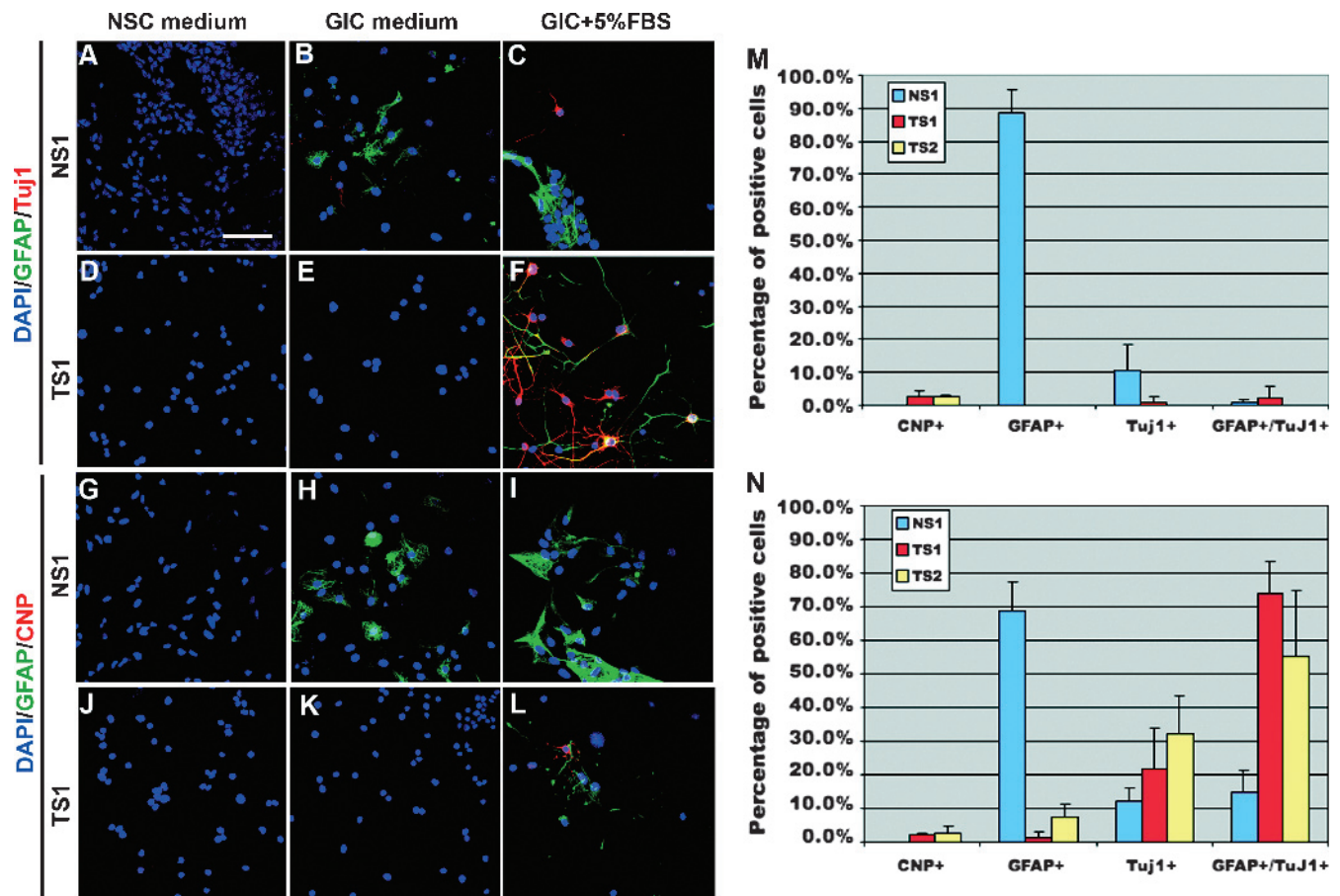


Figure 3. Expression of Tuj1, GFAP, and CNPase in representative samples of NS1 and TS1 cells cultured under different conditions for 7 days. Expression of GFAP and Tuj1 in NS1 (A–C) and TS1 (D–F) cells. Expression of GFAP and CNPase in NS1 (G–I) and TS1 (J–L) cells. Quantification of CNPase-, GFAP-, Tuj1-, and GFAP + Tuj1–positive cells in GIC medium (M) or GIC medium + 5% FBS (N). The experiment was repeated three times. Values represent the mean \pm SD. Scale bar, 50 μ m.

positive for both nestin and SOX2 (Figure 2, *A* and *D*). On EGF and FGF withdrawal (GIC medium) or in GIC medium with addition of 5% FBS, NS1 cells displayed an enlarged, flattened morphology and became negative for nestin (Figure 2, *B* and *C*). Also, SOX2 expression was clearly downregulated in the NS1 cells (Figure 2, *B* and *C*). In contrast, TS1 and TS2 cells retained the same levels of nestin and SOX2 in GIC medium compared to NSC medium (Figure 2*E*). On addition of 5% FBS to the GIC medium, TS1 and TS2 cells displayed the same enlarged morphology as the NS1 cells and became negative for nestin. SOX2 expression was, however, maintained in many cells (Figure 2*F*).

Next, we analyzed the expression of the neuronal marker Tuj1, the astrocytic marker GFAP, and the oligodendrocyte progenitor cell/oligodendrocyte marker CNPase in NSCs and GICs. GICs have been shown to exhibit abnormal differentiation abilities often resulting in cells that coexpress astrocytic and neuronal markers [7], which is rare for NSCs. NS1 cells that were cultured in NSC medium were negative for GFAP, CNPase, and Tuj1 (Figure 3, *A* and *G*). On EGF and FGF withdrawal or in GIC medium with 5% FBS, the number of GFAP- and Tuj1-positive cells increased, but there were no cells positive for CNPase (Figure 3, *B* and *C* and *H* and *I*). A quantification showed that, in GIC medium, 89% of NSCs were GFAP positive, 10% were Tuj1 positive, and only very few NS1 cells were GFAP and Tuj1 double positive (Figure 3*M*). Addition of 5% FBS

caused a decreased frequency of GFAP-positive cells (69%) and increased the frequency of GFAP and Tuj1 double positive cells to 15% (Figure 3*N*). The result from GICs showed that very few TS1 and TS2 cells expressed GFAP, Tuj1, and CNPase in NSC and GIC medium (Figure 3, *D–F* and *J–L*), indicating their stem cell-like state also under EGF- and FGF2-free conditions. By adding FBS to the medium, both TS1 and TS2 cells exhibited an altered GFAP and Tuj1 expression pattern compared with NS1 cells. Most cells (74% of TS1 and 82% of TS2) became double positive for GFAP and Tuj1 (Figure 3*N*). As for the NS1 cells, only rare CNPase single positive cells could be found.

Our data show that the GICs could maintain their stem cell-like properties when cultured as spheres in the absence of exogenous EGF and FGF2 and that they were capable of expressing multiple lineage markers on addition of FBS. However, their differentiation ability was abnormal, with a large proportion of cells being double positive for both astrocytic and neuronal markers, a feature that was rare in the serum-differentiated NSCs.

Serum-Induced Differentiation of GICs Was Reversible

The fact that most serum-differentiated GICs were double positive for GFAP and Tuj1 indicated that aberrant differentiation had occurred. Because terminal differentiation of GICs could be an avenue

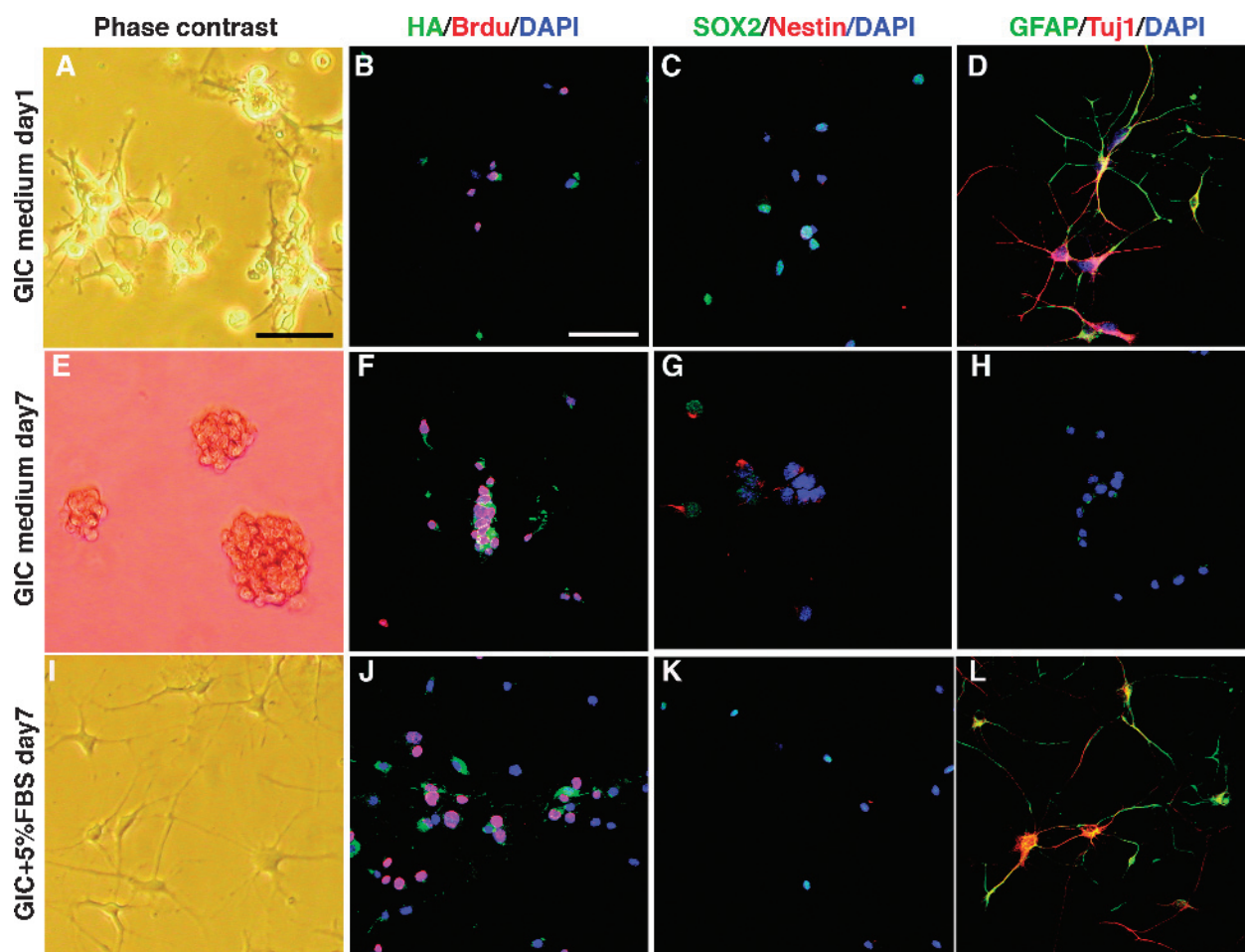
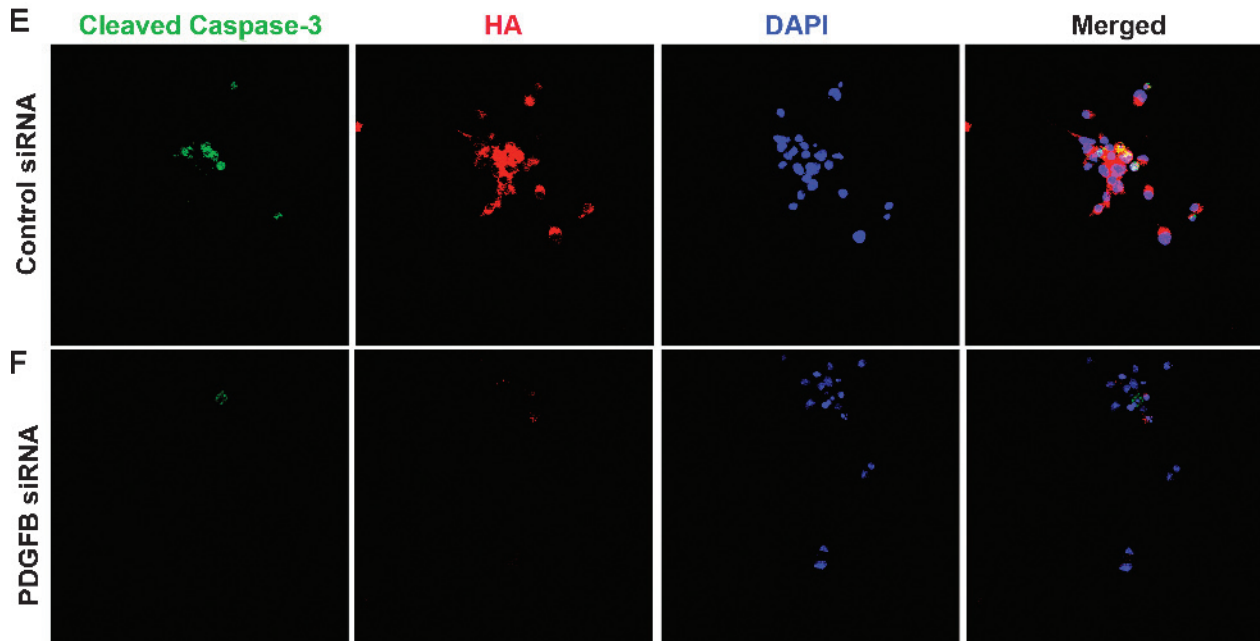
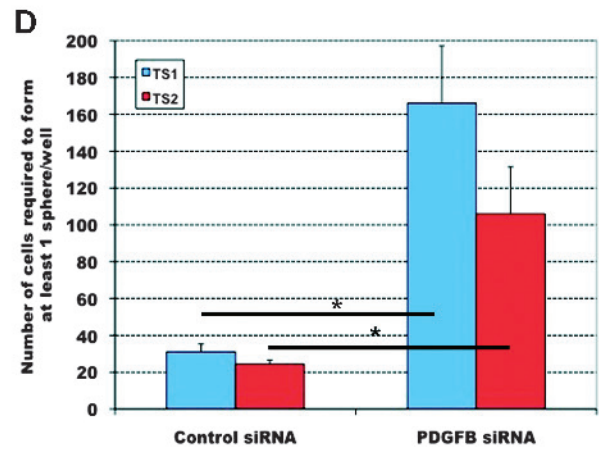
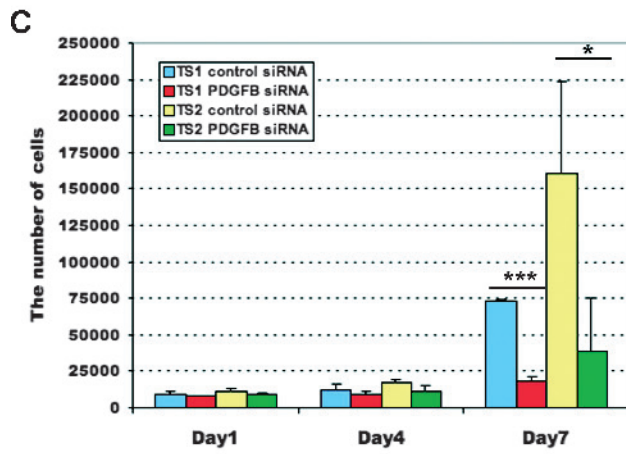
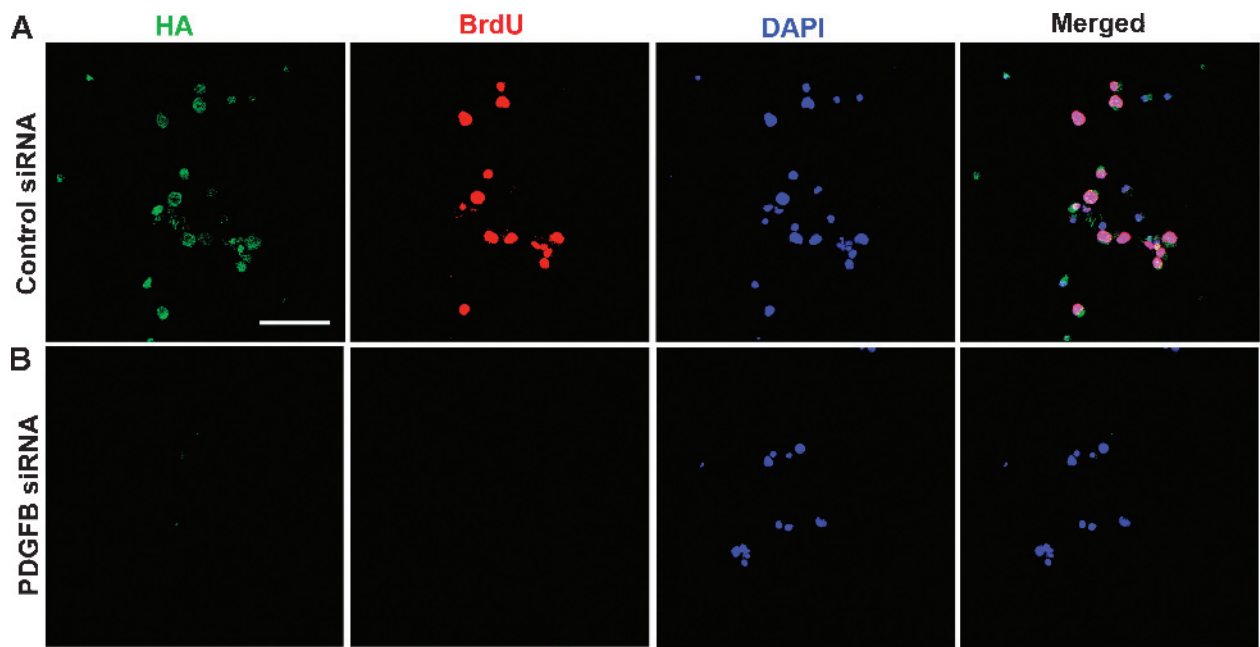


Figure 4. Reversibility of serum-induced differentiation of TS1 cells cultured in GIC medium + 5% serum for 7 days and after that in GIC medium for 24 hours (A-D), or GIC medium for 7 days (E-H), or GIC medium + 5% FBS (reference cells) for 7 days (I-L). (A, E, I) Phase-contrast showing cell morphology and expression of HA (tag on viral transduced PDGF-B) and BrdU (B, F, J), SOX2 and nestin (C, G, K), and GFAP and Tuj1 (D, H, L). Scale bar, 50 μ m.

for therapy, we were interested to analyze if this process was reversible or irreversible and to investigate if the serum-differentiated cells continued to proliferate. To test this, we used TS1 cells that had been cultured in GIC medium + 5% FBS for 7 days that displayed the typical enlarged, flattened morphology and put them back in GIC medium for 7 days. Already at day 1 in GIC medium, cells started to curl up and lose attachment to the dish (Figure 4A). All cells expressed the viral transduced human PDGF-B as analyzed by HA staining and approximately 50% of the cells were incorporating BrdU (Figure 4B). Barely any cells expressed Nestin, but SOX2 expression was retained in approximately 50% of the cells (Figure 4C) and most cells were strongly positive for GFAP and Tuj1 (Figure 4D). At day 7, TS1 cells had reverted entirely, and all cells grew as spheres (Figure 4E) and expressed PDGF-B (Figure 4F) and most cells were

BrdU positive (Figure 4F). Moreover, the cells had regained a high expression of Nestin and SOX2 (Figure 4G) and completely lost GFAP and Tuj1 expression (Figure 4H), indicating a complete reversion into a stem cell-like state again. Overall, they appeared indistinguishable to cells that had never been subjected to serum (Figure 2E). As reference cells, we used GICs that were maintained in GIC medium + 5% serum for another 7 days. These cells retained a differentiated morphology (Figure 4I), expressed GFAP and Tuj1 (Figure 4L), and were negative for nestin, as shown before (Figure 2F). However, the serum-differentiated TS1 cells were highly proliferative (Figure 4J) and continued to express PDGF-B (Figure 4J) and SOX2 (Figure 4K), although the PDGF-B expression was somewhat decreased in most cells, clearly establishing that serum could not induce terminal differentiation of our GICs.

Figure 5. Analysis of self-renewal, proliferation, and apoptosis on PDGF-B knockdown in GICs. (A-B) Expression of HA and BrdU in TS1 cells transfected with control (A) or PDGF-B (B) siRNA. (C) Total number of GICs after siRNA treatment. The experiment was repeated three times. Values represent the mean \pm SD. Student's *t* test, * P < 0.05, *** P < 0.001. (D) Stem cell frequency in GICs after the siRNA treatment. The experiment was repeated three times. Values represent the mean \pm SD. Student's *t* test, * P < 0.05. (E-F) Expression of cleaved Caspase-3 in TS1 cells treated with control (E) or PDGF-B (F) siRNA. Scale bar, 50 μ m.



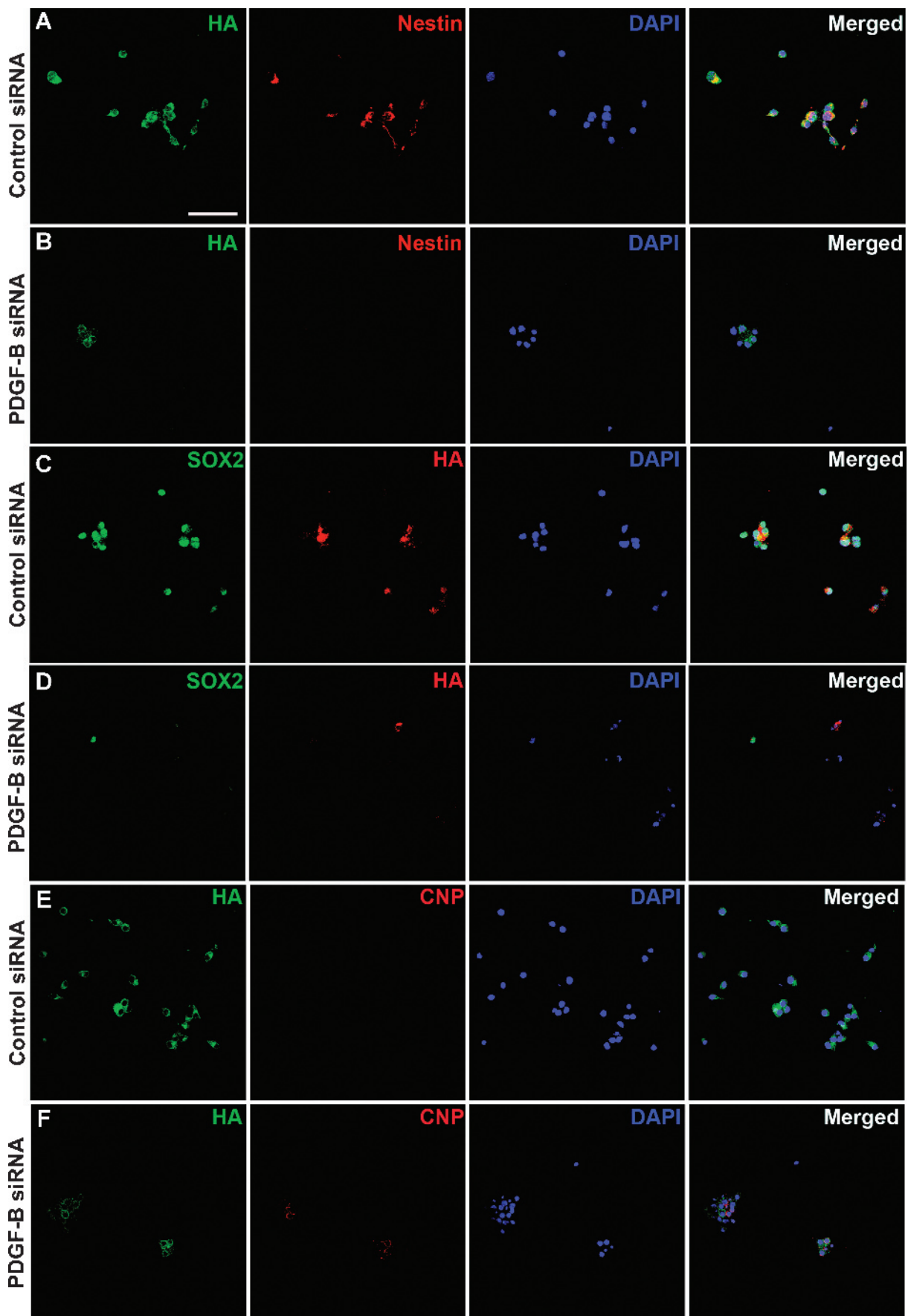


Figure 6. PDGF-B was indispensable for stemness of GICs. TS1 cells were treated with control or PDGF-B siRNA and expression of HA and nestin (A-B), HA and SOX2 (C-D), or HA and CNPase (E-F) were analyzed by double immunofluorescence staining. Scale bar, 50 μ m.

GIC Stemness Was Dependent on Expression of PDGF-B

To explore the relationship between PDGF-B expression and the stemness of GICs, we used siRNA against human PDGF-B to specifically reduce the viral transduced PDGF-B expression in TS1 cells. Immunostaining for HA was performed to analyze expression of viral transduced human PDGF-B protein (Figure 5, A and B). All TS1 cells transfected with control siRNA remained HA positive and 52% of the cells had incorporated BrdU (Figure 5A). In comparison, cells transfected with PDGF-B siRNA showed an obvious decrease in HA expression, and all HA-negative cells were also negative for BrdU incorporation (Figure 5B). However, the transfection efficiency was not complete, and there were occasional cells still expressing high levels of HA (data not shown). To further investigate the role of PDGF-B on the proliferation of GICs, TS1 and TS2 cells were seeded in fresh GIC medium 48 hours after the first siRNA transfection and the total cell number was counted on days 1, 4, and 7 (Figure 5C). The result showed that PDGF-B knockdown could significantly inhibit TS1 ($P < .001$) and TS2 ($P < .05$) cell proliferation when compared with control siRNA-treated cells (Figure 5C).

The role of PDGF-B for self-renewal ability of GICs was investigated by limiting dilution assay on siRNA-transfected cells. We found that inhibition of PDGF-B expression by siRNA could significantly reduce the stem frequency in both TS1 and TS2 cells (Student's t test, $P < .05$) compared with control siRNA-treated cells (Figure 5D).

Immunostaining for cleaved Caspase-3 was performed on control and PDGF-B siRNA-transfected cells to analyze whether the effects of PDGF-B knockdown on self-renewal and proliferation could be due to induction of apoptosis, but we could not find a correlation between PDGF-B down-regulation and cleaved Caspase-3 expression (Figure 5, E-F). To investigate if down-regulation of PDGF-B would lead to an effect on differentiation of GICs, we analyzed the expression of stem cell markers nestin and SOX2 together with expression of HA on PDGF-B knockdown. There was a significant and almost complete inhibition of both nestin (Figure 6B) and SOX2 (Figure 6D) expression in cells where HA was downregulated. There was no effect on nestin or SOX2 in control siRNA-treated cells (Figure 6, A and C). Expression of GFAP and Tuj1 was analyzed, but both control and PDGF-B siRNA-treated cells were found to be negative (data not shown). Interestingly, in cells where PDGF-B was downregulated, there was a uniform induction of CNPase expression (Figure 6F). This implies that the TS1 cells, when cultured under GIC condition, were kept in an early oligodendrocyte progenitor cell stage where the expression of PDGF-B is essential for maintenance of self-renewal.

PDGF-B Depletion Caused GICs to Lose Their Tumor-Initiating Capacity

The tumor-regenerating capacity of GICs depleted of PDGF-B was explored by the transfection of TS1 cells with control siRNA or PDGF-B siRNA followed by injections of 5000 treated cells intracranially into syngeneic newborn mice. Transfection of PDGF-B siRNA caused a significant inhibition of tumor development (Figure 7A). In the control siRNA group, all mice developed tumors, whereas there was a 50% tumor incidence in the PDGF-B siRNA group (Fisher exact test, $P = .044$). Histopathology analysis of tumors from the control siRNA (Figure 7B) and the PDGF-B siRNA (Figure 7C) groups both showed characteristics of high-grade glioma. PDGF-B expression was examined by HA staining, and notably, all the tumors from the control

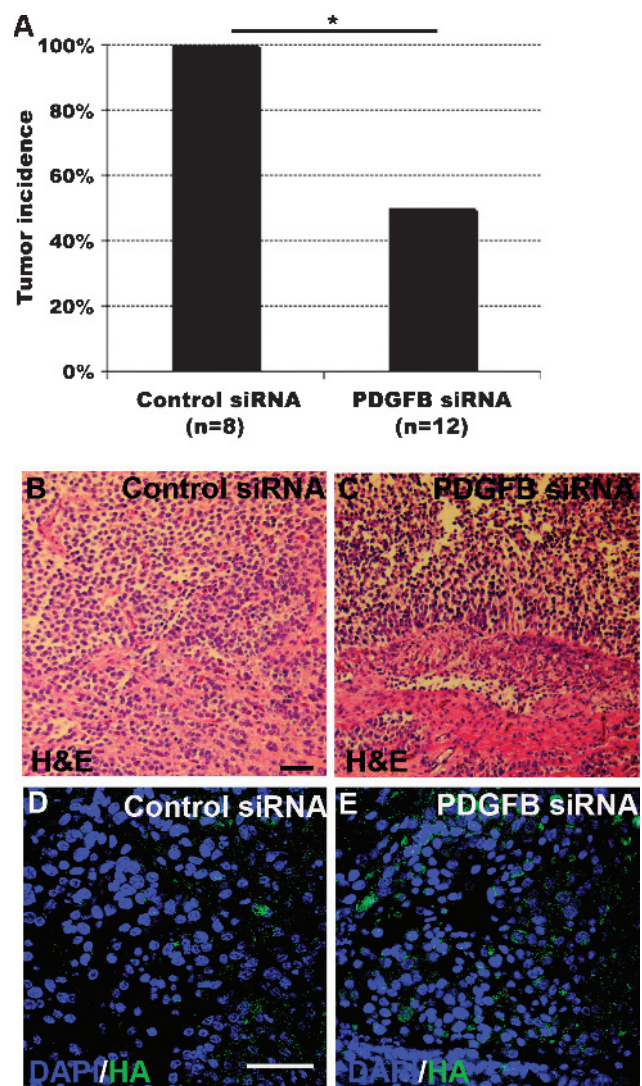


Figure 7. *In vivo* tumorigenic capacity of GICs was dependent on PDGF-B. (A) Tumor incidence in mice transplanted with TS1 cells treated with control or PDGF-B siRNA. Fisher exact test, $*P < 0.05$. (B and C) H&E staining of secondary tumors originated from control (B) or PDGF-B (C) siRNA-treated TS1 cells. Scale bar, 50 μ m. (D and E) HA staining of secondary tumors originated from control (D) or PDGF-B (E) siRNA-treated TS1 cells. Scale bar, 50 μ m.

siRNA group (Figure 7D) and the PDGF-B siRNA group (Figure 7E) were strongly positive for HA. The result suggested that the tumors that were formed from PDGF-B siRNA-transfected GICs originated from TS1 cells escaping the siRNA treatment, because we knew that as few as five GICs could generate a tumor and that the siRNA transfection efficiency was not complete.

Discussion

Several studies have shown that human glioma cell cultures will be enriched for CSCs/CICs that maintain the capacity to generate secondary tumors with the same phenotype and genotype as the original tumor when cultured under neurosphere conditions [5–7]. Because there is still a lack of specific and robust markers defining the CSC population, we have used the neurosphere culture protocol to isolate, characterize, and analyze the regulation of GICs derived from experimental gliomas with regard to self-renewal, proliferation, differentiation, and tumorigenicity.

We show that by culturing cells as spheres in growth factor-free medium, GICs can be derived and maintained from high-grade experimental gliomas and that these tumor cells exhibit all the current criteria defining CSCs/CICs. Most importantly, this culture condition was highly selective for tumor-initiating cells where as few as five cells were able to induce secondary tumors *in vivo* when orthotopically transplanted into syngeneic mice, and these tumors exhibited the histopathology and phenotype of the primary tumor. The potent tumor-initiating ability of the cells was supported by the result from the limiting dilution assay, which showed that the GIC cultures contained a high frequency of cells with self-renewal ability. Our findings show that experimental RCAS/TV-A-generated gliomas of the proneural-like subtype contain CSCs, corroborating a recent report showing that RCAS/TV-A-induced glioma cells with stem cell-like properties could be enriched in the side population cells [11].

In line with a study of human glioma cells, which showed that GICs could be cultured without addition of exogenous growth factors that was in part mediated by endogenous activation of EGFR signaling [16], we demonstrated that the experimental GICs driven by PDGF-B could proliferate and maintain their stemness without the addition of exogenous EGF and FGF2. However, in our case, addition of exogenous EGF and/or FGF2 to the medium did not confer an advantage for self-renewal of GICs, and in long-term cultures, GICs were negatively selected for in the presence of EGF and FGF2, indicating that NSCs have a faster growth rate than GICs. The reference cells used throughout the study were obtained by culturing normal NSCs under stem cell condition in defined medium with addition of EGF and FGF2. Initially, we made extensive efforts in setting up and culturing these cells under the same conditions as the GICs, in medium devoid of EGF and FGF2 but with addition of exogenous PDGF-BB, but found that the NSCs/glial progenitor cells could not be passaged under these conditions, neither as neurospheres nor as adherently cultured cells on ECM-coated dishes. These results point to the importance of selecting the appropriate culture conditions when maintaining GICs in long-term cultures.

We observed an abnormal differentiation capacity of GICs when subjected to serum-induced differentiation, where they mainly transitioned into cells coexpressing GFAP and Tuj1. This phenomenon of simultaneous expression of astrocytic and neuronal markers was rarely found in the normal NSCs that primarily were differentiated into astrocytes, likely due to the presence of bone morphogenetic proteins in the serum [17]. The coexpression of GFAP and Tuj1 could be a sign of malignancy because it has also been observed in human GICs [7]. It has been suggested that a disturbed differentiation capacity may even contribute to oncogenic transformation. In a somatic tumor suppressor model where neural stem/progenitor cells were genetically targeted to become *Pten*^{+/-} and *p53*^{-/-}, the target cells exhibited increased self-renewal capacity and aberrant differentiation properties before the appearance of visible tumors [18]. This could suggest that abnormal differentiation may serve as a prelude to tumor formation. Furthermore, we demonstrated that the aberrant serum-induced differentiation of GICs was reversible and that the cells could regain their stem cell-like state when cultured in GIC medium again. This *in vitro* phenotypic plasticity suggests that GICs may also change their phenotypes depending on the external tumor environment *in vivo*. Recently, it was shown that melanoma-derived cancer stem cells (CSCs) could display a dynamic phenotype. A group of slow-cycling melanoma cells with CSC characteristics was identified by JARID1B, whose expression was dynamically regulated by the external environ-

ment [19]. Depending on culture conditions, JARID1B-negative cells could give rise to different amount of JARID1B-positive progenies. Our results from experimental GICs are consistent with the findings in melanoma and suggest that, contradictory to the conventional unidirectional CSC model, the stemness of tumor cells may be dynamically related by the surrounding tumor niche.

We show that our experimental GICs are dependent on PDGF-B expression for self-renewal and proliferation *in vitro* and for tumorigenicity *in vivo*. The most obvious rationale for the PDGF dependence of experimental GICs is that the PDGF-B virus at tumor initiation caused a selection for target cells expressing PDGFRA and that the resulting autocrine/paracrine PDGF signaling in combination with *Arf* deficiency would be sufficient for GICs to occur. The presence of PDGFR- α in cultured tumor sphere cells supported this view. The results from the PDGF-B knockdown experiments suggest that PDGF signaling plays a role in regulating self-renewal of GICs, thus maintaining their stemness. In support, on specific PDGF-B down-regulation, all cells started to differentiate toward the oligodendrocytic cell lineage as indicated by uniform CNP expression. This feature has previously been observed for normal OPCs. In O-2A (oligodendrocyte/type 2 astrocyte) progenitor cells, which can give rise to oligodendrocytes *in vivo*, PDGF-B was shown to promote proliferation and motility and to prevent them from premature differentiation into oligodendrocytes [20]. Moreover, depletion of PDGF-B in the GICs significantly inhibited their tumor initiation capacity. This together with the fact that there were no HA-negative tumors among the secondary tumors strongly suggested that GICs were dependent on autocrine PDGF-B for tumorigenicity. Our results are in line with earlier data, which showed that when PDGF-B-induced tumor-bearing mice were treated with the PDGF-receptor inhibitor PTK787, the tumor cells stopped proliferating, but there was no sign of apoptosis [21]. The effect by PDGF inhibition on differentiation was not determined in these tumors.

In conclusion, we show that GICs are present in experimental gliomas in the RCAS/TV-A model, further supporting the relevance of this model system for the study of glioma. The experimental GICs were dependent on PDGF signaling for self-renewal, proliferation, and tumor initiation, and on inhibition of PDGF-B, cells stopped proliferating and started to uniformly differentiate into oligodendrocytes. Our results indicate that patients diagnosed with the proneural subtype of human glioma that are particularly insensitive to current therapies may benefit from drugs targeting signaling molecules regulating PDGF-controlled differentiation.

References

- Parsons DW, Jones S, Zhang X, Lin JC, Leary RJ, Angenendt P, Mankoo P, Carter H, Siu IM, Gallia GL, et al. (2008). An integrated genomic analysis of human glioblastoma multiforme. *Science* **321**, 1807–1812.
- TCGA (2008). Comprehensive genomic characterization defines human glioblastoma genes and core pathways. *Nature* **455**, 1061–1068.
- Verhaak RG, Hoadley KA, Purdom E, Wang V, Qi Y, Wilkerson MD, Miller CR, Ding L, Golub T, Mesirov JP, et al. (2010). Integrated genomic analysis identifies clinically relevant subtypes of glioblastoma characterized by abnormalities in PDGFRA, IDH1, EGFR, and NF1. *Cancer Cell* **17**, 98–110.
- Hemmati HD, Nakano I, Lazareff JA, Masterman-Smith M, Geschwind DH, Bronner-Fraser M, and Kornblum HI (2003). Cancerous stem cells can arise from pediatric brain tumors. *Proc Natl Acad Sci USA* **100**, 15178–15183.
- Singh SK, Clarke ID, Terasaki M, Bonn VE, Hawkins C, Squire J, and Dirks PB (2003). Identification of a cancer stem cell in human brain tumors. *Cancer Res* **63**, 5821–5828.
- Singh SK, Hawkins C, Clarke ID, Squire JA, Bayani J, Hide T, Henkelman RM, Cusimano MD, and Dirks PB (2004). Identification of human brain tumour initiating cells. *Nature* **432**, 396–401.

- [7] Galli R, Binda E, Orfanelli U, Cipelletti B, Gritti A, De Vitis S, Fiocco R, Foroni C, Dimeco F, and Vescovi A (2004). Isolation and characterization of tumorigenic, stem-like neural precursors from human glioblastoma. *Cancer Res* **64**, 7011–7021.
- [8] Beier D, Hau P, Proescholdt M, Lohmeier A, Wischhusen J, Oefner PJ, Aigner L, Brawanski A, Bogdahn U, and Beier CP (2007). CD133(+) and CD133(-) glioblastoma-derived cancer stem cells show differential growth characteristics and molecular profiles. *Cancer Res* **67**, 4010–4015.
- [9] Chen R, Nishimura MC, Bumbaca SM, Kharbanda S, Forrest WF, Kasman IM, Greve JM, Soriano RH, Gilmour LL, Rivers CS, et al. (2010). A hierarchy of self-renewing tumor-initiating cell types in glioblastoma. *Cancer Cell* **17**, 362–375.
- [10] Bao S, Wu Q, McLendon RE, Hao Y, Shi Q, Hjelmeland AB, Dewhirst MW, Bigner DD, and Rich JN (2006). Glioma stem cells promote radioresistance by preferential activation of the DNA damage response. *Nature* **444**, 756–760.
- [11] Bleau AM, Hambarzumyan D, Ozawa T, Fomchenko EI, Huse JT, Brennan CW, and Holland EC (2009). PTEN/PI3K/Akt pathway regulates the side population phenotype and ABCG2 activity in glioma tumor stem-like cells. *Cell Stem Cell* **4**, 226–235.
- [12] Tchougounova E, Kastemar M, Brasater D, Holland EC, Westermarck B, and Uhrbom L (2007). Loss of Arf causes tumor progression of PDGFB-induced oligodendroglioma. *Oncogene* **26**, 6289–6296.
- [13] Uhrbom L, Kastemar M, Johansson FK, Westermarck B, and Holland EC (2005). Cell type-specific tumor suppression by Ink4a and Arf in *Kras*-induced mouse gliomagenesis. *Cancer Res* **65**, 2065–2069.
- [14] Tropepe V, Sibilia M, Ciruna BG, Rossant J, Wagner EF, and van der Kooy D (1999). Distinct neural stem cells proliferate in response to EGF and FGF in the developing mouse telencephalon. *Dev Biol* **208**, 166–188.
- [15] Aboody KS, Brown A, Rainov NG, Bower KA, Liu S, Yang W, Small JE, Herrlinger U, Ourednik V, Black PM, et al. (2000). Neural stem cells display extensive tropism for pathology in adult brain: evidence from intracranial gliomas. *Proc Natl Acad Sci USA* **97**, 12846–12851.
- [16] Kelly JJ, Stechishin O, Chojnacki A, Lun X, Sun B, Senger DL, Forsyth P, Auer RN, Dunn JF, Cairncross JG, et al. (2009). Proliferation of human glioblastoma stem cells occurs independently of exogenous mitogens. *Stem Cells* **27**, 1722–1733.
- [17] Mabie PC, Mehler MF, Marmur R, Papavasiliou A, Song Q, and Kessler JA (1997). Bone morphogenetic proteins induce astroglial differentiation of oligodendroglial-astroglial progenitor cells. *J Neurosci* **17**, 4112–4120.
- [18] Alcantara Llaguno S, Chen J, Kwon CH, Jackson EL, Li Y, Burns DK, Alvarez-Buylla A, and Parada LF (2009). Malignant astrocytomas originate from neural stem/progenitor cells in a somatic tumor suppressor mouse model. *Cancer Cell* **15**, 45–56.
- [19] Roesch A, Fukunaga-Kalabis M, Schmidt EC, Zabierowski SE, Brafford PA, Vultur A, Basu D, Gimotty P, Vogt T, and Herlyn M (2010). A temporarily distinct subpopulation of slow-cycling melanoma cells is required for continuous tumor growth. *Cell* **141**, 583–594.
- [20] Noble M, Murray K, Stroobant P, Waterfield MD, and Riddle P (1988). Platelet-derived growth factor promotes division and motility and inhibits premature differentiation of the oligodendrocyte/type-2 astrocyte progenitor cell. *Nature* **333**, 560–562.
- [21] Uhrbom L, Nerio E, and Holland EC (2004). Dissecting tumor maintenance requirements using bioluminescence imaging of cell proliferation in a mouse glioma model. *Nat Med* **10**, 1257–1260.

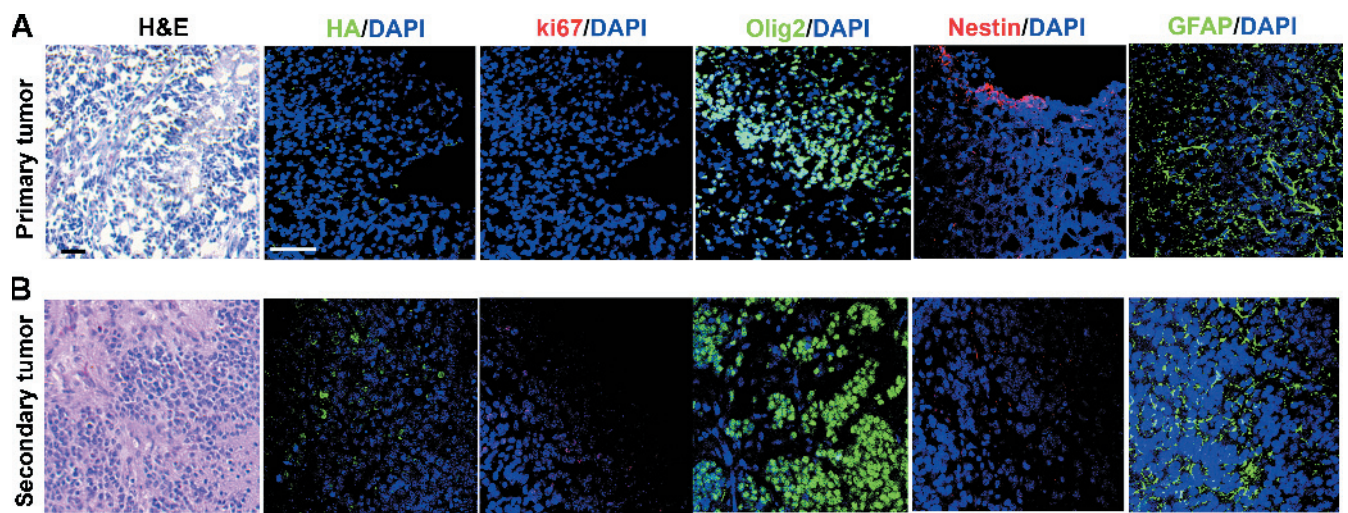


Figure W1. H&E and immunofluorescence stainings for HA, Ki67, Olig2, Nestin, and GFAP in sections from primary (A) and secondary (B) gliomas. Scale bar, 50 μ m.